Cellulose (2014) 21:291–299
DOI 10.1007/s10570-013-0124-z

ORIGINAL PAPER

Properties of poly(acrylamide)/TEMPO-oxidized cellulose nanofibril composite films

Takanori Kurihara · Akira Isogai

Received: 26 September 2013 / Accepted: 19 November 2013 / Published online: 3 December 2013

Abstract Self-standing composite films consisting of 2,2,6,6-tetramethylpiperidine-1-oxyl-oxidized cellulose nanofibril (TOCN) and anionic poly(acrylamide) (PAM) in various weight ratios were prepared by casting and drying of homogeneous mixtures of aqueous TOCN dispersion and PAM solution. PAM/TOCN composite films consisting of 25 % PAM and 75 % TOCN had clearly higher Young's modulus (13.9 GPa) and tensile strength (266 MPa) than 100 % TOCN film (10.8 GPa and 223 MPa, respectively) or 100 % PAM film (4.9 GPa and 78 MPa, respectively), showing that PAM molecules have mechanical reinforcement ability in TOCN matrix. Some attractive interactions are likely formed between TOCN element surfaces and PAM molecules. In contrast, no such mechanical improvements were observed for poly(vinyl alcohol)/TOCN or oxidized starch/TOCN composite films prepared as references. Moreover, the mechanical properties of the PAM/TOCN composite films were further improved by controlling molecular mass and branching degree of the PAM. The high optical transparency and low coefficient of thermal expansion of the 100 % TOCN film were mostly maintained in the TOCN composite film containing 25 % PAM.

Keywords TEMPO-oxidized cellulose nanofibril · Poly(acrylamide) · Composite film · Mechanical properties · Mechanical reinforcement

T. Kurihara · A. Isogai (✉)
Graduate School of Agricultural and Life Sciences, The University of Tokyo, 1-1-1 Yayoi, Bunkyo-ku, Tokyo 113-8657, Japan
e-mail: aisogai@mail.ecc.u-tokyo.ac.jp

T. Kurihara
R&D Company, Harima Chemicals Inc., 671-4 Mizuashi, Noguchi-cho, Kakogawa, Hyogo 675-0019, Japan

Introduction

In this century, fundamental and application studies of nanocelluloses, i.e., cellulose nanocrystals (CNCs) and nanofibrillated celluloses (NFCs), have been rapidly expanding. Nanocelluloses have advantages as bio-based nanomaterials compared with other currently high-profile nanomaterials such as metal nanowires, electrospun nanofibers, carbon nanotubes, and graphenes. First, new apparatus such as grindstone-type homogenizers, water collision-type homogenizers, and new microfluidizers have been developed to efficiently convert wood cellulose fibers suspended in water to highly fibrillated NFCs (Isogai 2013). Second, several pretreatments of wood celluloses have been reported to reduce the energy consumption of NFC preparation during mechanical disintegration treatment in water, such as mild endoglucanase treatment, carboxymethylation, cation polymer-addition, esterification, and oxidation. These pretreatments also allow the degree of nanofibrillation

of NFCs to be increased (Klemm et al. 2011; Isogai et al. 2011; Isogai 2013), decreasing the energy consumption of their preparation.

Because NFCs prepared using only mechanical treatment in water or in combination with enzymatic and carboxymethylation pretreatments have high crystallinities, Young's modulus, tensile strengths, and surface areas, and form network structures in aqueous dispersions and dried materials, self-standing films, coating layers, foams, and composites of NFCs have advantageous and unique properties in terms of mechanical strength, optical transparency, thermal stability, and gas-barrier performance (Henriksson et al. 2008; Eichhorn et al. 2009; Siqueira et al. 2010; Siró and Plackett 2010; Sehaqui et al. 2010, 2011; Liu et al. 2011).

We have developed 2,2,6,6-tetramethylpiperidine-1-oxy radical (TEMPO)-mediated oxidation as a pretreatment to convert wood cellulose fibers to completely individualized TEMPO-oxidized cellulose nanofibrils (TOCNs) with homogeneous widths of $\approx$3 nm dispersed in water (Saito et al. 2006, 2007; Isogai et al. 2011). Anionic sodium carboxylate groups are densely and regularly present on TOCN element surfaces, with the result that osmotic effects and electrostatic repulsion act efficiently between the anionically charged TOCN elements both during mild mechanical disintegration treatment in water and in the subsequent dispersed state (Okita et al. 2010; Hirota et al. 2010). TOCN elements maintaining sufficiently nano-dispersed states in matrix polymers, the individual TOCN elements will efficiently mechanically reinforce TOCN/polymer composites (Li et al. 2010) owing to the high Young' modulus ($\approx$140 GPa) and ultimate tensile strength (1–3 GPa) of TOCNs (Iwamoto et al. 2009; Saito et al. 2013). However, because TOCNs are highly hydrophilic owing to abundant sodium carboxylate groups, some surface-treatments of TOCNs must first be carried out to efficiently develop nanocomposite effects in hydrophobic matrix polymers such as poly(styrene) and poly(L-lactide) (Johnson et al. 2011; Bulota and Hughes 2012; Bulota et al. 2012; Fujisawa et al. 2013).

Because the original TOCN elements are individually dispersed in water, TOCN-containing composites are more easily prepared with water-soluble polymers or water-dispersible nanoclays through drying of the aqueous mixtures. When poly(vinyl alcohol) or hydroxypropyl cellulose was used as a water-soluble polymer matrix with TOCNs, nanocomposite behavior was observed for TOCN-containing composite films and fibers prepared under certain conditions (Johnson et al. 2009; Endo et al. 2013). Montmorillonite-TOCN composite films and layer-by-layer coated films of TOCN/chitin nanofibrils, prepared using water as a co-dispersion media, showed unique mechanical, optical, and oxygen-barrier properties (Wu et al. 2012; Qi et al. 2012).

Poly(acrylamide) (PAM) is another water-soluble synthetic polymer. Nonionic, anionic, cationic, and amphoteric PAMs with various molecular masses, charge densities, and branching degrees have been synthesized to obtain suitable performance as dry strength additives or retention aids for the wet-end process of papermaking (Yoshimoto et al. 2004; Wang et al. 2006; Baraki 2013). Because PAM molecules have abundant C=O and NH_2 groups, both of which can form hydrogen bonds with cellulosic fibers, PAM molecules may also contribute to the mechanical reinforcement of TOCN films when PAM/TOCN composite films are fabricated under suitable conditions. Moreover, because sodium carboxylate groups and hydroxyl groups are present in high density on TOCN element surfaces, both C=O and NH_2 groups present in each PAM repeating unit are expected to form attractive interactions with such functional groups of TOCN surfaces, which may improve the mechanical properties of PAM/TOCN composite films.

In this study, therefore, PAM/TOCN composite films were fabricated by casting and drying of homogeneous mixtures of PAM solution and TOCN dispersion with various weight ratios. The mechanical, optical, and thermal properties of the films were characterized to elucidate the mechanical reinforcement behaviors of PAM molecules with various molecular masses and branching degrees in TOCN matrix, with the aim of designing suitable PAM/TOCN composite films for various end uses.

Experimental

Materials

A commercially available softwood bleached kraft pulp (SBKP) for papermaking (Nippon Paper Co., Ltd., Tokyo, Japan) was used as the original wood

cellulose (Shinoda et al. 2012). The SBKP was soaked in 0.1 M HCl at room temperature for 2 h for demineralization, and then washed through repeated filtration with water. A 50 % aqueous solution of acrylamide was purchased from Mitsui Chemicals, Inc. (Tokyo, Japan). Poly(vinyl alcohol) (PVA: JF-17, saponification degree >98 %, Japan Vam & Poval Co. Ltd., Osaka, Japan) and oxidized starch (MS #3800, Nihon Shokuhin Kako Co. Ltd., Tokyo, Japan) were used as 0.15 % (w/w) aqueous solutions after dissolution in water through adequate heat treatment. All other reagents were purchased from Wako Pure Chemical (Osaka, Japan) and used as received.

Preparation of TOCN/water dispersion

A TEMPO-oxidized cellulose was prepared from SBKP according to a previously reported method (Shinoda et al. 2012), in which a TEMPO/NaBr/NaClO system with 5.0 mmol NaClO per gram of SBKP was used in water at pH 10 and room temperature. The TEMPO-oxidized cellulose thus obtained was post-oxidized with $NaClO_2$ in an acetate buffer at pH 4.8 for conversion of the small amount of C6-aldehydes present in the TEMPO-oxidized cellulose to C6-carboxyl groups. The obtained TEMPO-oxidized cellulose had a carboxylate content of 1.40 mmol g^{-1}, as determined by conductivity titration (Saito and Isogai 2004). An aqueous 0.15 % (w/w) slurry of the TEMPO-oxidized cellulose was disintegrated using a blender-type homogenizer (Excel Auto ED-4, Nissei, Japan) at 15,000 rpm for 5 min, and subsequently sonicated at 19.5 kHz and 300 W output power with a 26 mm probe tip (US-300T, Nissei, Japan) for 6 min to prepare a TOCN/water dispersion. The dispersion was then centrifuged at 12,000*g* for 20 min to remove unfibrillated or partly fibrillated fraction. The nanofibrillation yields of the TOCN/water dispersions were approximately 95 %.

Preparation of aqueous PAM solutions

PAMs were synthesized in water through free-radical polymerization from acrylamide with small amounts of an ionic monomer and a branching agent. Milli-Q water was used in all PAM synthesis experiments. A typical procedure was as follows. An aqueous 50 % acrylamide solution (77 g), 98 % acrylic acid (4.5 g), sodium methallylsulfonate (0.1 g), sodium hydroxide (2.2 g), and water (300 g) were placed into a four-necked flask equipped with a reflux condenser, and the mixture was heated to 60 °C in a nitrogen atmosphere. Then, an aqueous 0.5 % ammonium persulfate solution (10 g) was added to the mixture, which was allowed to react at 85 °C for 2 h. An anionic 9.8 % PAM solution was obtained after the reaction was quenched by inhibitor addition and cooled to room temperature. Other PAMs with different molecular masses and branching degrees were prepared by adding different amounts of reagents or under different conditions.

Preparation of PAM/TOCN, PVA/TOCN, and starch/TOCN composite films

An aqueous 0.15 % TOCN dispersion and a 0.15 % PAM, PVA, or starch solution were blended in various weight ratios at pH 6–7, and the mixture was stirred for at least 30 min and then degassed through centrifugation. The mixture was then poured into a poly(styrene) petri dish, and dried at 40 °C for 2 days. The self-standing, approximately 10 μm thick PAM/TOCN, PVA/TOCN, and starch/TOCN composite films thus obtained were conditioned at 23 °C and 50 % relative humidity (RH) for more than 1 day before analyses.

Analyses of polymers

The molecular mass parameters of the PAMs, PVA, and starch were measured by size-exclusion chromatography (SEC) with right angle-laser light scattering (RALLS). The SEC conditions were as follows: 0.1 % (w/w) sample concentration, 500 μL injection volume, 0.8 mm min^{-1} flow rate, and column temperature of 40 °C. A guard column (PWXL; Tosoh, Japan) and two SEC columns packed with a cross-linked methacrylate polymer gel (GMPWXL; Tosoh) were used. The detector cells were kept at 40 °C. The sample solution and eluent (0.05 M phosphate buffer at pH 6.8) were filtered through 1.0 and 0.3 μm disposable membranes (Advantec Toyo Ltd., Japan), respectively, before analysis. The electrical charges of the polymers were determined using colloidal titration; 10 mg of 0.05 % aqueous PAM solution was titrated using a poly-ionic titrant with an opposite charge to that of the sample, using a Mütek PCD-04 streaming current detector (Germany). The cationic and anionic titrants used were 0.0025 N poly(diallyldimethylammonium

chloride) and potassium poly(vinyl sulfate), respectively.

Analyses of composite films

Light transmittance spectra of the PAM/TOCN composite films were measured using a UV–Vis spectrophotometer (JASCO, V-670, Japan). The thickness of the films was calculated from the interference patterns that appeared in their transmittance and/or reflectance spectra obtained using a JASCO analysis program, according to a previously reported method (Lin and Chen 2009). The refractive indices of the PAM/TOCN composite films used for calculation of film thickness were 1.55, which was measured at 589 nm wavelength using an Abbe refractometer (Atago, NAR-1T SOLID, Tokyo, Japan) with the sodium D-line. The surface morphology of the films was observed using a Nanoscope IIIa atomic force microscope (AFM: Veeco Instruments, USA) in tapping mode. Tensile tests of the approximately 10 μm thick films were carried out using a Shimadzu EZ-TEST tensile tester with a 500 N load cell and a 10 mm span length. Specimens in 30 and 2 mm length and width, respectively, were measured at 1 mm min^{-1}, and at least 10 specimens were measured for each sample. The moisture content of films conditioned at 23 °C and 50 % RH were calculated gravimetrically from their dried weights obtained after vacuum drying at room temperature for 12 h. The thermal expansivity of the films was determined using a Shimadzu TMA-60 instrument. The measurements were performed on films dried at 120 °C for 10 min to remove the residual water present in the original films in a nitrogen atmosphere at 0 % RH under a 0.03 N load, at temperatures from 30 to 120 °C with a heating rate of 5 °C min^{-1}.

Results and discussion

Preparation of PAM/TOCN composite films

It has been reported that aqueous TOCN dispersions consist of completely individualized TOCN elements, and thus have high light-transmittances and show birefringence when observed between cross-polarizers (De Souza Lima and Borsali 2004; Isogai et al. 2011). Self-standing TOCN films prepared from aqueous TOCN dispersions through casting and drying also have high light-transmittances (Saito et al. 2006; Fukuzumi et al. 2009).

In this study, self-standing PAM/TOCN composite films of various weight ratios were first prepared using an anionic PAM, which had weight-average and number-average molecular masses, a radius of gyration, and a charge density of 2,060,000, 404,000, 57.8 nm, and −1.06 meq g^{-1}, respectively. Thus, the PAM and TOCN used both had anionic charges in water at pH $\approx$ 7. In preliminary experiments, it was found that the homogeneous TOCN dispersion turned to a gel on addition of a cationic PAM, owing to formation of cross-linking between the anionic TOCN elements and cationic PAM molecules. In contrast, the anionic PAM/TOCN dispersion was flowable and highly transparent without any formation of gel particles, and the resulting PAM/TOCN composite film was transparent as well (Fig. 1a–c). All the PAM/TOCN composite films, irrespective of the PAM/TOCN weight ratios, had high light-transmittances of $\approx$90 % at 600 nm. The clear interferences of the UV–Vis spectra observed for all composite films (Fig. 1c) indicate high smoothness of the film surfaces and uniformity of the film thickness over large surface areas (Takahashi et al. 2009; Wu et al. 2012; Fukuzumi et al. 2013). The AFM images showed that the film surfaces consisted of randomly-oriented TOCN elements. Because the morphological sharpness of TOCN elements were similar between the two AFM images (Fig. 1d), it was difficult to conclude from these AFM images alone that each TOCN element was partly covered with PAM molecules in the PAM/TOCN composite film.

Properties of PAM/TOCN, PVA/TOCN, and starch/TOCN composite films

The self-standing PAM/TOCN, PVA/TOCN, and starch/TOCN composite films were prepared from homogeneous dispersions of various polymer/TOCN weight ratios. The moisture content and film density of the composite films are depicted in Fig. 2. Moisture contents of 100 % PAM and starch films were higher than that of the 100 % TOCN film, indicating that PAM and starch molecules formed disordered structures in the films and had groups much more accessible to moisture than those in the 100 % TOCN film. In contrast, the PVA sample, which has a lower

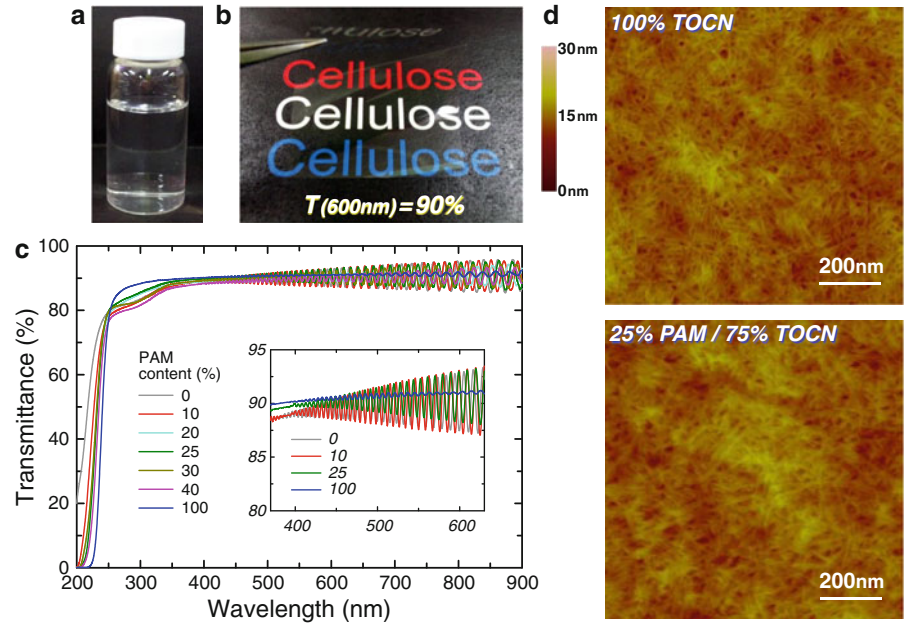

Fig. 1 An aqueous PAM/TOCN (25:75 by weight) dispersion (**a**), its cast and dried film (**b**), UV–Vis spectra of PAM/TOCN composite films (**c**), and surface AFM images of PAM/TOCN films (**d**)

molecular mass than those of PAM and starch, as described later, may form somewhat ordered structures owing to its lower molecular mass (Endo et al. 2013), resulting in lower moisture contents of the PVA/TOCN composite films with increasing PVA content. The density of PAM/TOCN and PVA/TOCN composite films decreased with increasing polymer content, while that of starch/TOCN films was roughly constant. These density data may reflect pore volumes in the composite films.

Typical strain–stress curves of the composite films are shown in Fig. 3, and the Young's modulus and tensile strength of the composite films are summarized in Fig. 4a, b, respectively. The 100 % TOCN film had remarkably high Young's modulus and tensile strength, 10.8 GPa and 223 MPa, respectively, compared with those of 100 % PAM, 100 % PVA, and 100 % starch film, which were lower than 5 GPa and 80 MPa, respectively. This is because TOCN film consists of nanoelements with high aspect ratios (>200) and high crystallinity (≈75 %) (Iwamoto et al. 2009; Fukuzumi et al. 2009; Saito et al. 2013).

It is noteworthy that the Young's modulus and tensile strength of the TOCN film were clearly increased by compositing with 10 and 25 % PAM, while no such improvement of mechanical properties was observed for the PVA/TOCN or starch/TOCN composite films. In particular, the Young's modulus, tensile strength, and yield stress of the TOCN film were raised by averages of 29, 19 and 58 %, respectively, for the 25 % PAM/75 % TOCN composite film. Thus, only the PAM sample among the polymers used in this study was found to have a characteristic TOCN matrix reinforcement ability, although both PVA and starch molecules have numerous hydroxyl groups which may also have the potential to form hydrogen bonds with hydroxyl groups present on TOCN surfaces.

These results indicate that some attractive interactions formed at the interfaces between TOCN element surfaces and PAM molecules in the composite films, while no such interactions existed in the PVA/TOCN or starch/TOCN composite films. The specific reinforcement behavior of the 25 % PAM/75 % TOCN composite film may partly be explainable in terms of the surface charges of the two components; the PAM molecules and TOCN elements used had anionic charges of 1.06 meq g^{-1} and 1.4 mmol g^{-1}, respectively. Suitable electrostatic repulsions present between anionic PAM molecules and anionic TOCN elements in both the dispersed state and during the drying process may have brought about sufficient nano-dispersion of the TOCN elements without aggregation in the dried films. Similar results have also been observed for montmorillonite/TOCN composite films, in which both the nanoclay particles and

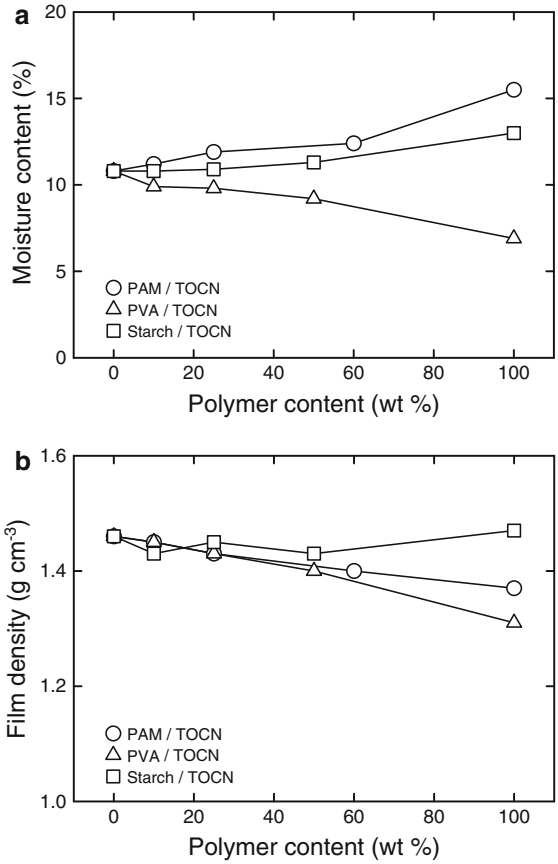

Fig. 2 Moisture content (**a**) and density (**b**) of PAM/TOCN, PVA/TOCN, and starch/TOCN composite films with various polymer content

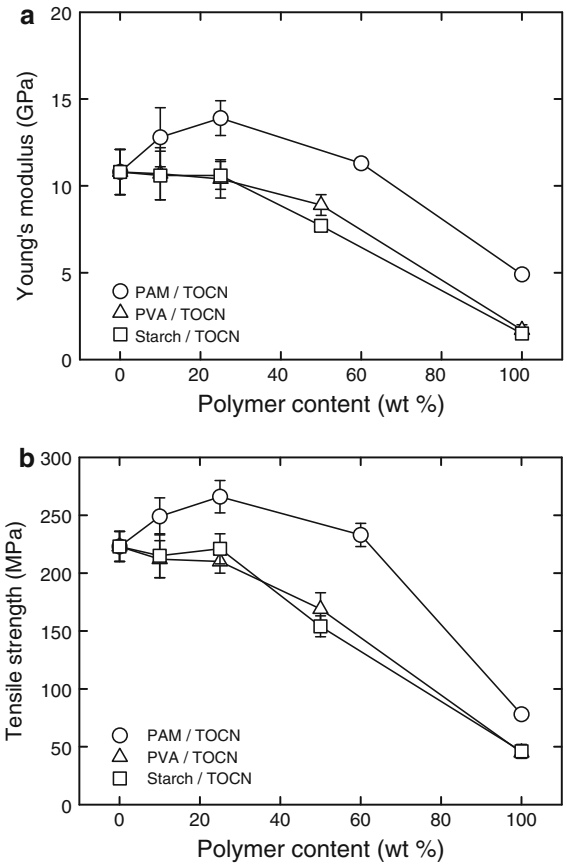

Fig. 4 Young's modulus (**a**) and tensile strength (**b**) of PAM/TOCN, PVA/TOCN, and starch/TOCN composite films with various polymer content

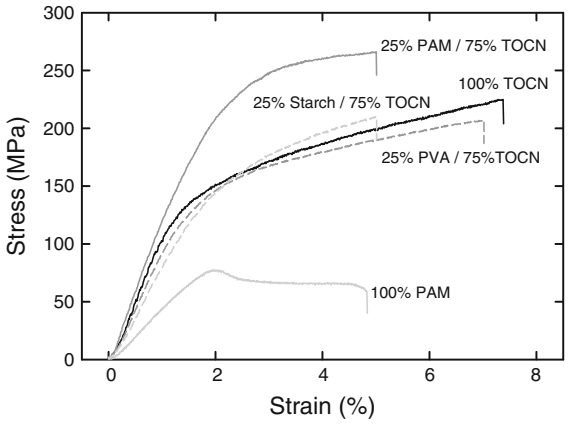

Fig. 3 Typical strain–stress curves of 100 % TOCN, 25 % PAM/75 % TOCN, 100 % PAM, 25 % PVA/75 % TOCN, and 25 % starch/75 % TOCN composite films

the TOCN elements had anionic surface charges (Wu et al. 2012).

The characteristic chemical structure of PAM may also participate in the mechanism for the mechanical reinforcement of the TOCN matrix; the amide structure of the C=O and NH_2 groups in each repeating unit of PAM can form hydrogen bonds with the hydroxyl groups of TOCN surfaces. Moreover, these polar functional groups may also form attractive interactions with dissociated carboxylate groups abundantly present on TOCN surfaces, while the hydroxyl groups of PVA or starch molecules cannot form such positive interactions with sodium carboxylate groups on the TOCN surfaces.

Figure 5a, b show the elongation at break and work of fracture, respectively, of the composite films. The elongation at break decreased with increasing polymer content in the films up to 50–60 %, indicating mostly

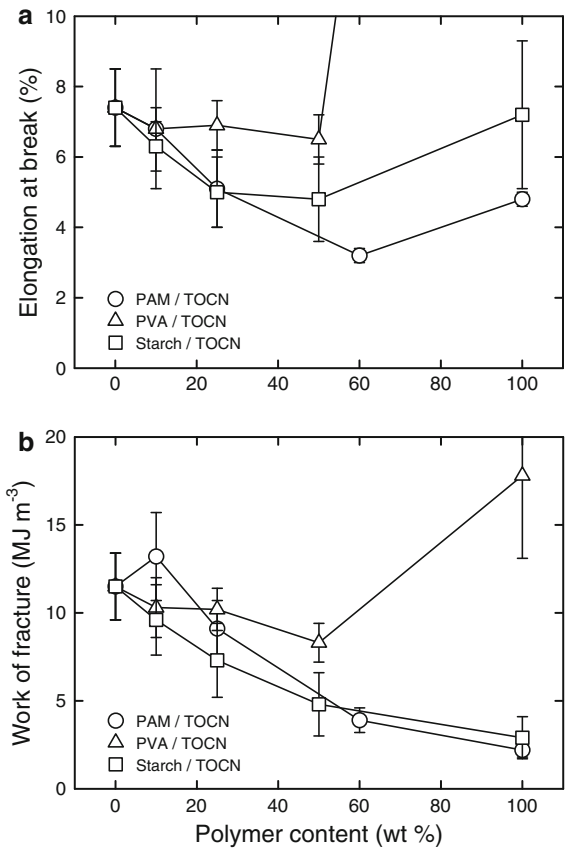

Fig. 5 Elongation at break (**a**) and work of fracture (**b**) of PAM/TOCN, PVA/TOCN, and starch/TOCN composite films with various polymer content

diminished ductile properties for these composite films. However, the 100 % polymer films had elongations at break greater than those of the composite films containing 50–60 % polymer. Especially, the 100 % PVA film had an extremely large elongation at break of ≈48 %. The work of fracture was increased only for the 10 % PAM/90 % TOCN composite film (from 11.5 to 13.2 MJ m^{-3}), whereas the other composite films had lower work of fractures than that of the 100 % TOCN film. Thus, most of the composite films were rather brittle, although the detailed mechanism explaining these results is unknown at present.

The thermal expansion behavior of the PAM/TOCN composite films was also measured. The coefficients of thermal expansion (CTEs) of the 100 % TOCN and the 25 % PAM/75 % TOCN films had similar values of 5.6 and 6.4 ppm K^{-1}, respectively. These low CTE values resulted from the high crystallinity of the TOCN elements (Nishino et al. 2004; Abe et al. 2007; Fukuzumi et al. 2009), and hence the low CTE value of TOCN was mostly maintained in the 25 % PAM/75 % TOCN composite film.

Effects of molecular mass parameters of PAMs, PVA, and starch on properties of composite films

It is well known that the molecular masses, branching degrees, and charge densities of PAMs used as wet-end additives in papermaking sensitively influence their retention behavior and the resultant mechanical properties of PAM-containing paper and board (Yoshimoto et al. 2004; Hubbe 2006; Wang et al. 2006; Baraki 2013). Hence, we synthesized various PAM samples with different molecular masses and branching degrees, and studied their mechanical reinforcement behavior in PAM/TOCN composite films. The relationships between weight-average molecular mass (M_w) and radius of gyration (R_g) of the synthesized PAMs as well as the PVA and starch samples, determined by SEC-RALLS, are shown in Fig. 6.

The synthesized PAM samples are classified into two groups depending on their branching degrees; low- and highly-branched PAMs. These two PAM groups were synthesized by controlling the amount of the branching agent added. 25 % PAM/75 % TOCN composite films were then prepared using these samples, and their mechanical properties were evaluated in terms of the M_w values of the PAMs (Fig. 7).

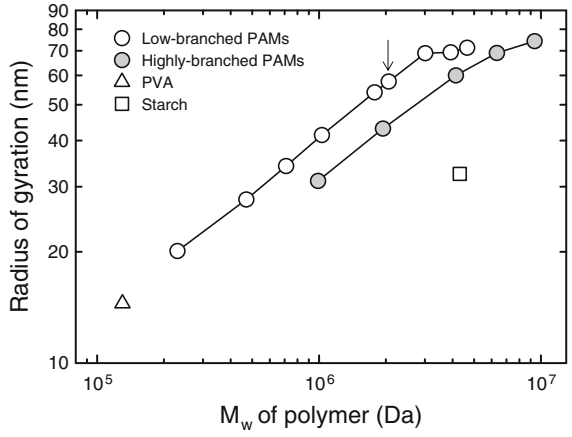

Fig. 6 Relationships between molecular mass and radius of gyration of low-branched and highly-branched PAMs, PVA, and starch used in this study. *Arrow* indicates the PAM sample used in Figs. 1, 2, 3, 4, 5

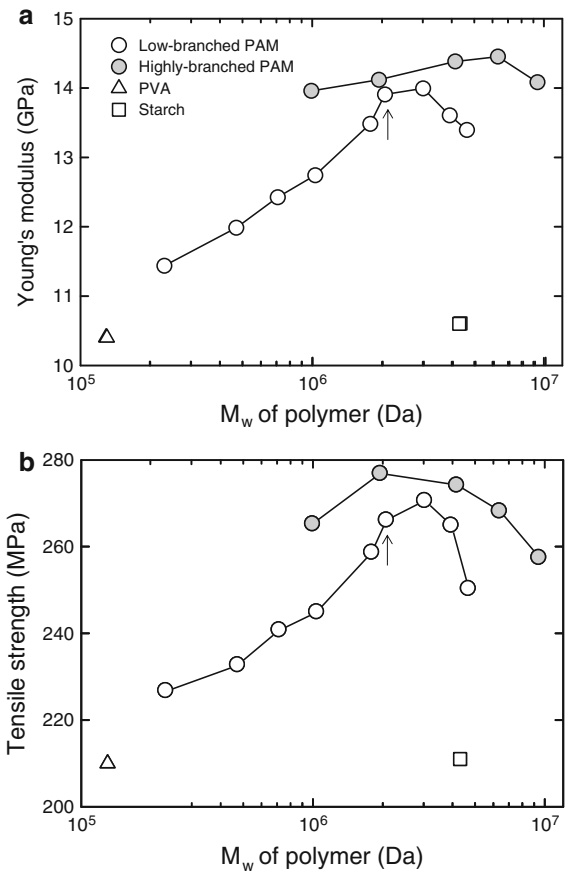

Fig. 7 Effects of weight-average molecular mass of low-branched and highly-branched PAMs on Young's modulus (**a**) and tensile strength (**b**) of PAM/TOCN composite films. *Arrow* indicates the PAM sample used in Figs. 1, 2, 3, 4, 5

When low-branched PAMs were used, both the Young's modulus and tensile strength of the 25 % PAM/75 % TOCN composite films increased with PAM M_w, and exhibited maximum values at around 2–3 MDa. PAMs with higher M_w than these rather decreased both the Young's modulus and tensile strength, showing that optimal PAM M_w values exist for the mechanical reinforcement of TOCN. Moreover, the highly-branched PAMs gave higher Young's modulus and tensile strength to the composite films than the low-branched PAMs, when compared at similar M_w. Consequently, the molecular mass values of the PAMs greatly influenced the resultant mechanical properties of the composite films. The low Young's modulus and tensile strength of the PVA/TOCN film in Fig. 5 are partly explainable in terms of the low M_w of the PVA used, whereas the results for the starch/TOCN composite film could not be elucidated in terms of M_w alone.

Conclusion

Aqueous solutions of anionic PAM, PVA, or oxidized starch were homogeneously mixed with TOCN dispersions without forming any aggregates, providing highly transparent self-standing polymer/TOCN composite films after casting/drying of the mixtures. The PAM/TOCN composite films had high light-transmittances of $\approx$90 % at 600 nm wavelength, irrespective of PAM content from 10 to 60 %, showing that the TOCN elements maintained their nano-dispersed state in the composite films. Both the Young's modulus and tensile strength of the TOCN film were improved by compositing with 25 % PAM of 2–3 MDa in M_w, while its high optical transparency and thermal stability were mostly unchanged. In contrast, no such mechanical reinforcement behavior was observed for PVA/TOCN or starch/TOCN composite films. Thus, some attractive interactions may form at the interfaces between TOCN surfaces and PAM molecules of 2–3 MDa, particularly at around 25 % PAM content. However, no such interactions exist between TOCN elements and either PVA or starch molecules. The anionic charge and/or the specific amide structure in each repeating unit of the PAM molecules may have brought about the clear mechanical reinforcement of the TOCN matrix. Because the molecular mass, charge density, and branching degree of PAMs are controllable within our current synthesis technologies, which have been accumulated in production of various PAMs used as wet-end additives in papermaking, it is possible to design the present PAM/TOCN composite films to have adequate mechanical properties for various end uses.

Acknowledgments This research was supported by a Grant-in-Aid for Scientific Research (Grant No. 21228007) from the Japan Society for the Promotion of Science (JSPS).

References

Abe K, Iwamoto S, Yano H (2007) Obtaining cellulose nanofibers with a uniform width of 15 nm from wood. Biomacromolecules 8:3276–3278

Baraki H (2013) Structure-control of amphoteric polyacrylamide and its performance as dry strength resin. Jpn Tappi J 67(5):544–549

Bulota M, Hughes M (2012) Toughening mechanisms in poly(lactic) acid reinforced with TEMPO-oxidized cellulose. J Mater Sci 47:5517–5523

Bulota M, Tanpichai S, Hughes M, Eichhorn SJ (2012) Micromechanics of TEMPO-oxidized fibrillated cellulose composites. ACS Appl Mater Interfaces 4:331–337

De Souza Lima MM, Borsali R (2004) Rodlike cellulose microcrystals: structure, properties, and applications. Macromol Rapid Commun 25:771–787

Eichhorn SJ, Dufresne A, Aranguren M, Marcovich NE, Capadona JR, Rowan SJ, Weder C, Thielemans W, Roman M, Rennecker S, Gindl W, Veigel S, Keckes J, Yano H, Abe K, Nogi M, Nakagaito AN, Mangalam A, Simonsen J, Benight AS, Bismarck A, Berglund LA, Peijs T (2009) Review: current international research into cellulose nanofibers and nanocomposites. J Mater Sci 45:1–33

Endo R, Saito T, Isogai A (2013) TEMPO-oxidized cellulose nanofibril/poly(vinyl alcohol) composite drawn fibers. Polymer 54:935–941

Fujisawa S, Saito T, Kimura S, Iwata T, Isogai A (2013) Surface engineering of ultrafine cellulose nanofibrils toward polymer nanocomposite materials. Biomacromolecules 14:1541–1546

Fukuzumi H, Saito T, Iwata T, Kumamoto Y, Isogai A (2009) Transparent and high gas barrier films of cellulose nanofibers prepared by TEMPO-mediated oxidation. Biomacromolecules 10:162–165

Fukuzumi H, Fujisawa S, Saito T, Isogai A (2013) Selective permeation of hydrogen gas using cellulose nanofibril film. Biomacromolecules 14:1705–1709

Henriksson M, Berglund LA, Isaksson P, Lindström T, Nishino T (2008) Cellulose nanopaper structures of high toughness. Biomacromolecules 9:1579–1585

Hirota M, Furihata K, Saito T, Kawada T, Isogai A (2010) Glucose/glucuronic acid alternating co-polysaccharides prepared from TEMPO-oxidized native celluloses by surface peeling. Angew Chem Int Ed 49:7670–7672

Hubbe MA (2006) Bonding between cellulosic fibers in the absence and presence of dry-strength agents—a review. Bioresources 1:281–318

Isogai A (2013) Wood nanocelluloses: fundamentals and applications as new bio-based nanomaterials. J Wood Sci. doi:10.1007/s10086-013-1365-z

Isogai A, Saito T, Fukuzumi H (2011) TEMPO-oxidized cellulose nanofibers. Nanoscale 3:71–85

Iwamoto S, Kai W, Isogai A, Iwata T (2009) Elastic modulus of single cellulose microfibrils from tunicate measured by atomic force microscopy. Biomacromolecules 10:2571–2576

Johnson RK, Zink-Sharp A, Renneckar SH, Glasser WG (2009) A new bio-based nanocompoiste: fibrillated TEMPO-oxidized celluloses in hydroxypropylcellulose matrix. Cellulose 16:227–238

Johnson RK, Zink-Sharp A, Glasser WG (2011) Preparation and characterization of hydrophobic derivatives of TEMPO-oxidized nanocelluloses. Cellulose 18:1599–1609

Klemm D, Kramer F, Moritz S, Lindström T, Ankerfors M, Gray D, Dorris A (2011) Nanocelluloses: a new family of nature-based materials. Angew Chem Int Ed 50:5438–5466

Li Z, Renneckar S, Barone JR (2010) Nanocomposites prepared by in situ enzymatic polymerization of phenol with TEMPO-oxidized nanocellulose. Cellulose 17:57–68

Lin KM, Chen YY (2009) Improvement of electrical properties of sol–gel derived ZnO: Ga films by infrared heating method. J Sol Gel Sci Technol 51:215–221

Liu A, Walther A, Ikkala O, Belova L, Berglund LA (2011) Clay nanopaper with tough cellulose nanofiber matrix for fire retardancy and gas barrier functions. Biomacromolecules 12:633–641

Nishino T, Matsuda I, Hirao K (2004) All-cellulose composite. Macromolecules 37:7683–7687

Okita Y, Saito T, Isogai A (2010) Entire surface oxidation of various cellulose microfibrils by TEMPO-mediated oxidation. Biomacromolecules 11:1696–1700

Qi ZD, Saito T, Fan Y, Isogai A (2012) Multifunctional coating films by layer-by-layer deposition of cellulose and chitin nanofibrils. Biomacromolecules 13:553–558

Saito T, Isogai A (2004) TEMPO-mediated oxidation of native cellulose. The effect of oxidation conditions on chemical and crystal structures of the water-insoluble fractions. Biomacromolecules 5:1983–1989

Saito T, Nishiyama Y, Putaux JL, Vignon M, Isogai A (2006) Homogeneous suspensions of individualized microfibrils from TEMPO-catalyzed oxidation of native cellulose. Biomacromolecules 7:1687–1691

Saito T, Kimura S, Nishiyama Y, Isogai A (2007) Cellulose nanofibers prepared by TEMPO-mediated oxidation of native cellulose. Biomacromolecules 8:2485–2491

Saito T, Kuramae R, Wohlert J, Berglund LA, Isogai A (2013) An ultrastrong nanofibrillar biomaterial: the strength of single cellulose nanofibrils revealed via sonication-induced fragmentation. Biomacromolecules 14:248–253

Sehaqui H, Liu A, Zhou Q, Berglund LA (2010) Fast preparation procedure for large, flat cellulose and cellulose/inorganic nanopaper structures. Biomacromolecules 11:2195–2198

Sehaqui H, Zhou Q, Berglund LA (2011) Nanostructured biocomposites of high toughness—a wood cellulose nanofiber network in ductile hydroxyethylcellulose matrix. Soft Matter 7:7342–7350

Shinoda R, Saito T, Okita Y, Isogai A (2012) Relationship between length and degree of polymerization of TEMPO-oxidized cellulose nanofibrils. Biomacromolecules 13:842–849

Siqueira G, Bras J, Dufresne A (2010) Cellulosic bionanocomposites: a review of preparation, properties and applications. Polymers 2:728–765

Siró I, Plackett D (2010) Microfibrillated cellulose and new nanocompoiste materials: a review. Cellulose 17:459–494

Takahashi M, Iyoda K, Miyauchi T, Ohkido S, Tahashi M, Wakita K, Kajitani N, Kurachi M, Hotta K (2009) Preparation and characterization of Eu: Ti codoped $LiNbO_3$ films prepared by the sol–gel method. J Appl Phys 106:044102

Wang Y, Hubbe MA, Sezaki T, Wang X, Rojas OL, Argyropoulos DS (2006) The role of polyampholyte charge density on its interactions with cellulose. Nord Pulp Paper Res J 21:638–645

Wu CN, Saito T, Fujisawa S, Fukuzumi H, Isogai A (2012) Ultrastrong and high gas-barrier nanocellulose/clay-layered composites. Biomacromolecules 13:1927–1932

Yoshimoto Y, Iwasa Y, Fujiwara T (2004) Study on the mechanism of PAMs as paper dry strength agents. Proceeding of the 71st Pulp and Paper Research Conference, pp 123–125